Available potential energy gain from mixing due to the nonlinearity of the equation of state in a global ocean model

L. S. Urakawa,[1] J. A. Saenz,[2] and A. M. Hogg[2,3]

Received 10 March 2013; revised 25 April 2013; accepted 25 April 2013; published 31 May 2013.

[1] Densification in the ocean interior upon mixing at high latitudes, due to the nonlinear equation of state (EoS) of seawater, enhances the meridional overturning circulation (MOC). However, recent calculations using numerical simulations of global ocean circulation have shown that the nonlinearity of the EoS leads to a sink of gravitational potential energy (PE), from which one might infer that there is less energy available to be released to the MOC. Here the available PE (APE) budget of the global ocean is investigated using a numerical model with a nonlinear EoS under a realistic configuration. The results show that, while the nonlinearity of the EoS leads to a loss of gravitational PE, it is a source of APE. For the model used in this study, nonlinearity of the EoS is as significant as surface buoyancy forcing in generating APE. **Citation:** Urakawa, L. S., J. A. Saenz, and A. M. Hogg (2013), Available potential energy gain from mixing due to the nonlinearity of the equation of state in a global ocean model, *Geophys. Res. Lett.*, *40*, 2224–2228, doi:10.1002/grl.50508.

1. Introduction

[2] The meridional overturning circulation (MOC) involves dense water formation in polar regions and upwelling distributed over other areas. This circulation transports heat and nutrients in large quantities and is considered to have a large impact on climate. Considerable attention has been paid to the driving mechanisms and energetics of the MOC in recent years. Maintaining this circulation requires a source of kinetic energy (KE) on the global scale to overcome viscous dissipation. There are two energy sources: direct KE input by winds and energy conversion from gravitational potential energy (hereafter PE) on the scale of general circulation. *Toggweiler and Samuels* [1998], *Gnanadesikan et al*. [2005] and *Urakawa and Hasumi* [2009] conduct numerical experiments with ocean general circulation models under realistic configurations and find that in the global energy budget, large amounts of KE are converted to PE (although this does not necessarily imply the absence of any energy conversions from PE to KE). The latter study also shows that this conversion from KE to PE is in part due to Ekman upwelling and downwelling. Ekman upwelling (downwelling) under a stable stratification pulls up (pushes down) isopycnal surfaces. Both lead to raising the center of gravity and PE gain. *Urakawa and Hasumi* [2009] experiment with enhanced winds in the Southern Ocean to investigate the effects of winds on the MOC. They eliminate the wind effect in the Atlantic by calculating basin-wise energy budget anomalies by comparing experiments with and without enhanced winds in the Southern Ocean and find that PE is converted to KE in order to compensate the local viscous dissipation of KE associated with the enhanced Atlantic MOC.

[3] It is also important to consider sinks of PE because they restrict the energy that can be converted to KE. *Urakawa and Hasumi* [2010] show that over 100 GW of PE is consumed by "cabbeling" in their model ("cabbeling" there also includes the thermobaric effect [e.g., *McDougall*, 1984]. Refer to the auxiliary material for further information.). This result seems to imply that the nonlinear effects of the equation of state (EoS) might work to weaken the circulation by reducing PE and the subsequent conversion from PE to KE. On the other hand, *Urakawa and Hasumi* [2012] diagnose the water mass transformation rate due to cabbeling in an eddy-resolving model of the Southern Ocean. About 3 Sv of Lower Circumpolar Deep Water is modified into Antarctic Bottom Water (AABW) on the continental slopes of Antarctica in their model. This source of AABW is notably large compared to the estimates of formation rates which range from 10 to 20 Sv [*Orsi et al*., 1999; *Hellmer and Beckmann*, 2001; *Naveira Garabato et al*., 2002; *Kusahara et al*., 2010]. *Klocker and McDougall* [2010] also show that the nonlinearity of the EoS leads to a significant amount of dense water formation in the Southern Ocean. These results support the expectation that the effects of the nonlinearity should strengthen the MOC.

[4] This apparent discrepancy between the nonlinear effects of the EoS on the energy budget and on the overturning circulation may be resolved using the available PE (APE) framework. APE is the amount of PE that is available to be converted to KE. It is defined as the difference between PE and background PE (BPE), which is the minimum PE state achieved by sorting water masses adiabatically [*Lorenz*, 1955]. This BPE amounts to a large fraction of PE which is not available to drive motion. Earlier studies focusing on the APE budget of the MOC [*Huang*, 1998; *Toggweiler and Samuels*, 1998] have demonstrated inconsistencies with a PE budget analysis. For example, diapycnal mixing is a source of PE but often leads to an energy sink in the APE framework. *Hughes et al*. [2009] and *Tailleux* [2009] outline a new APE framework which is consistent with the PE budget by including BPE and separately

Additional supporting information may be found in the online version of this article.

[1]Atmosphere and Ocean Research Institute, University of Tokyo, Kashiwa, Chiba, Japan.
[2]Research School of Earth Sciences, Australian National University, Canberra, ACT, Australia.
[3]ARC Centre of Excellence for Climate System Science, Australian National University, Canberra, ACT, Australia.

Corresponding author: L. S. Urakawa, Atmosphere and Ocean Research Institute, University of Tokyo, 5-1-5, Kashiwanoha, Kashiwa-shi, Chiba, Japan. (surakawa@aori.u-tokyo.ac.jp)

0094-8276/13/10.1002/grl.50508

discussing reversible stirring and irreversible mixing. The APE theory has provided valuable insights into driving mechanisms of the MOC. *Saenz et al*. [2012] showed that the ocean energetics and circulation are actively modulated by surface buoyancy and wind forcing and that the power input from each forcing has a positive feedback on the other.

[5] The effects of the nonlinearity of the EoS on APE have not been well investigated. Dense water formation due to this nonlinearity could enhance the baroclinicity of the density distribution, generating a source of APE, despite being a sink of PE. This could resolve the discrepancy between the nonlinear effects of the EoS on PE and on the MOC. However, the dependency of density on pressure in a fully nonlinear EoS makes it difficult to calculate the BPE. Here we use an approximate method proposed by *Huang* [2005]. This method goes well with the EoS adopted in our model which depends upon depth rather than pressure. This study is the first attempt to quantitatively investigate the nonlinear effects of the EoS on APE in a global ocean model.

2. Model Configuration

[6] The model employed for this study is COCO, version 4 [*Hasumi*, 2006]. This model is based on the primitive equations under the hydrostatic and Boussinesq approximations with an explicit free surface and is formulated using a general orthogonal, curvilinear horizontal coordinate frame with the geopotential height as the vertical coordinate. The model configuration is the same as in *Urakawa and Hasumi* [2010] except for the EoS and the integration time. It is a global ocean model, with horizontal resolution of about 300 km at low latitudes and 100 km at high latitudes. The model has 33 levels with spacing ranging from 50 m at the top and 200 m at the bottom. Sea surface temperature and salinity are restored to the monthly climatological values of World Ocean Atlas 2005 [*Locarnini et al*., 2006; *Antonov et al*., 2006], and the monthly average of *Röske*'*s* [2001] wind climatology is imposed. The isopycnal tracer diffusivity and layer thickness diffusivity are $1\times10^{3}\,\mathrm{m^{2}s^{-1}}$ and $3\times10^{2}\,\mathrm{m^{2}s^{-1}}$, respectively. We adopt vertical diffusivity of *Tsujino et al*. [2000] case 3 (0.1–$3.0\times10^{-4}\,\mathrm{m^{2}s^{-1}}$). The model is run for 4011 years, and a set of 10 day interval snapshots from the last year is analyzed.

3. Energetics Framework

[7] This study employs the EoS of *McDougall et al*. [2003], with $\rho=\rho(\theta,s,p(z))$, where ρ is in situ density and θ, s, and p are potential temperature, salinity, and pressure, respectively. Pressure for the EoS is calculated as a function of depth, $p=-\rho_0 gz$ where $\rho_0 g=10^{4}\mathrm{Nm}^{-2}$. The reference level is set at the mean sea surface as discussed in *Urakawa and Hasumi* [2009]. The temporal and spatial derivatives of density can be written as

$$\begin{aligned}\frac{\partial\rho}{\partial t}&=\rho_\theta\frac{\partial\theta}{\partial t}+\rho_s\frac{\partial s}{\partial t},\ \nabla_h\rho=\rho_\theta\nabla_h\theta+\rho_s\nabla_h s,\ \frac{\partial\rho}{\partial z}\\&=\rho_\theta\frac{\partial\theta}{\partial z}+\rho_s\frac{\partial s}{\partial z}+\rho_p\frac{\mathrm{d}p(z)}{\mathrm{d}z},\end{aligned}\tag{1}$$

where $\nabla_h=(\partial/\partial x,\partial/\partial y,0)$ and ρ_θ, ρ_s, and ρ_p are defined by $(\partial\rho/\partial\theta)_{s,p}$, $(\partial\rho/\partial s)_{\theta,p}$, and $(\partial\rho/\partial p)_{\theta,s}$, respectively. Substituting advection-diffusion equations for θ and s into the equation for the temporal derivative of density, multiplying it by gravitational acceleration and depth, and integrating over the domain, we obtain the following PE budget

$$\begin{aligned}\frac{\mathrm{d}E_p}{\mathrm{d}t}&=\int_V gz\frac{\partial\rho}{\partial t}\mathrm{d}V\\&=\Phi_{b1}+\left[\Phi'_z+\overline{\Phi_z}+\Phi_z^{\mathrm{GM}}\right]+\left[\Phi_c^{v}+\Phi_c^{i}+\Phi_c^{n}\right]+\Phi_g\\&\quad+\Phi_{vi}+\Phi_{\mathrm{ca}},\end{aligned}\tag{2}$$

where $E_p=\int_V\rho gz\mathrm{d}V$ is the gravitational PE of the system and V is the volume of the model domain. The terms on the right-hand side of equation (2) represent surface buoyancy forcing; the rates of energy exchange with TKE (turbulent kinetic energy), MKE (KE associated with the mean flow), and eddy KE (EKE); sinks of PE due to the nonlinearity of the EoS from vertical, isopycnal, and numerical diffusion; vertical dependency of EoS; vertical isopycnal diffusion; and convective adjustment, respectively, and are written in the auxiliary material in more detail.

[8] The strategy for achieving the minimum PE state (used to determine BPE) is described as follows [*Huang*, 2005]. Our model has 33 layers, and each layer has a reference pressure. First, the in situ density of all ocean grid points is calculated using the reference pressure of the 33rd layer and sorted. Then, we stack grid points in the 33rd layer, beginning with the densest, until the layer is full. Next, density profiles of unstacked grid points are recalculated with the reference pressure of the 32nd layer. Grid points are sorted and stacked in the same way, and we continue this procedure until all layers have been filled. This method tries to put an ocean grid point with heavier density on a deeper level, which leads to a lower PE state.

[9] The in situ density of a fluid parcel in the reference state (ρ^*) is, in general, different from its original density, ρ, due to compressibility. The depth of a water mass after sorting (z^*) therefore cannot be expressed in analytical form, leading to an expression for BPE that is different from the one obtained in *Winters et al*. [1995]. BPE of the system is given by $E_b=\int_V\rho^* gz^*\mathrm{d}V$, and its tendency is evaluated as follows:

$$\frac{\mathrm{d}E_b}{\mathrm{d}t}=\int_V gz^*\frac{\partial\rho}{\partial t}\mathrm{d}V+\int_V\left[\rho g\frac{\partial z^*}{\partial t}+\frac{\partial}{\partial t}(gz^*\delta\rho)\right]\mathrm{d}V,\tag{3}$$

where $\delta\rho=\rho^*-\rho$. The second integral in equation (3) appears because of the dependency of density on pressure (depth in this study). The first term in the right-hand side is the same as the term discussed in *Hughes et al*. [2009], and is evaluated as

$$\begin{aligned}\int_V gz^*\frac{\partial\rho}{\partial t}\mathrm{d}V&=\Phi_{b2}+\left[\Phi_d^{v}+\Phi_d^{i}+\Phi_d^{n}\right]+\left[\hat{\Phi}_c^{v}+\hat{\Phi}_c^{i}+\hat{\Phi}_c^{n}\right]\\&\quad+\Phi_{\mathrm{GM}}+\hat{\Phi}_{\mathrm{ca}}.\end{aligned}\tag{4}$$

[10] The nine terms on the right-hand side are APE gain by surface buoyancy forcing; APE loss due to irreversible mixing owing to vertical, isopycnal, and numerical diffusion; sinks due to the nonlinear effects of the EoS from vertical, isopycnal, and numerical diffusion; GM (Gent and McWilliams) parameterization; and convective adjustment, respectively. The terms with a hat take the same form as the terms without hat in PE equation except that the depth is z^*. Further information about abbreviations are found in the auxiliary material.

[11] APE is defined as the difference between PE and BPE, $E_a=E_p-E_b$. The effect of cabbeling, which is a major

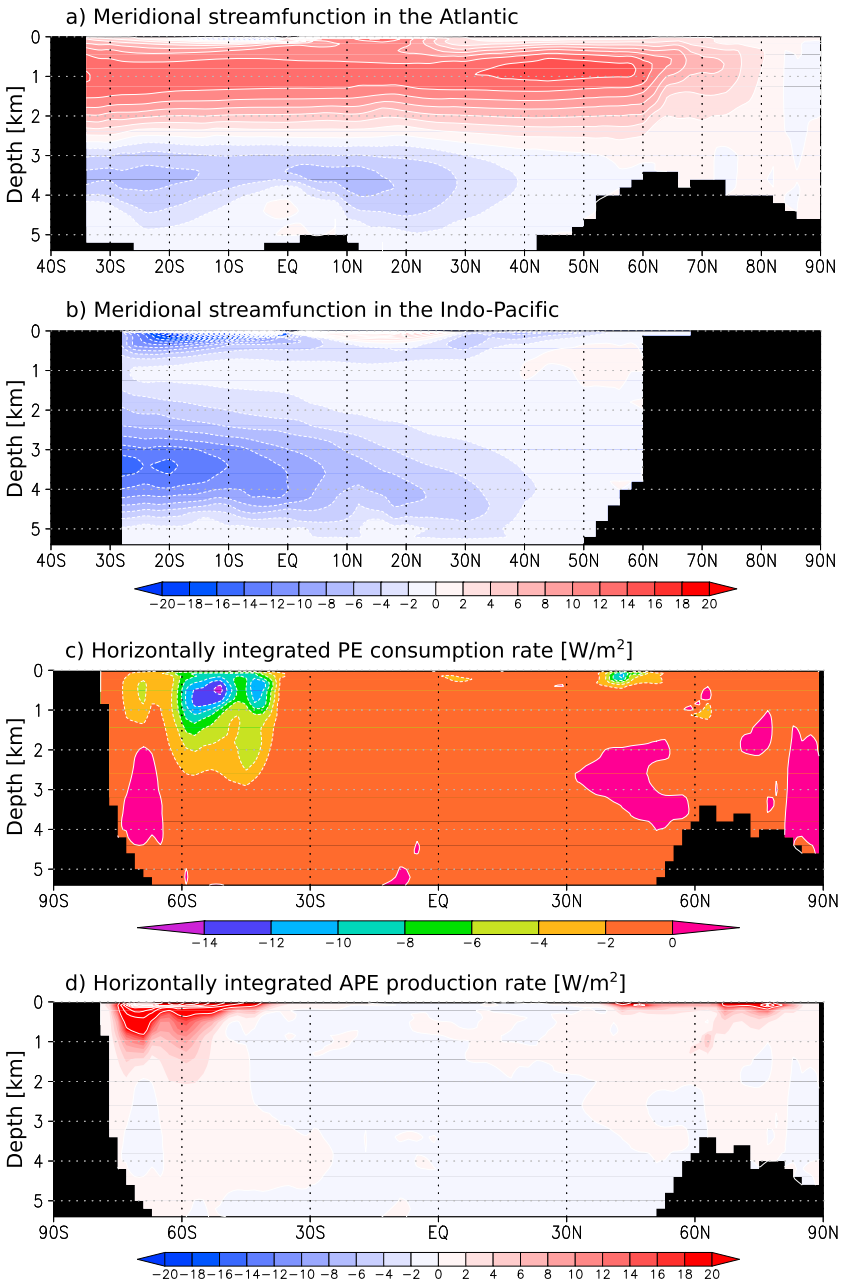

Figure 1. Meridional views of the model results. Meridional stream function in (a) the Atlantic and (b) the Indo-Pacific. Global zonally integrated (c) PE consumption and (d) APE production rates due to the nonlinear effects of the EoS associated with isopycnal diffusion. Contour intervals are 2 Sv for Figures 1a and 1b, 2 Wm^{-2} for Figure 1c, and 20 Wm^{-2} for Figure 1d.

component of the nonlinear effect of the EoS, on the APE budget is evaluated to be $g(z-z^*)C$, where C denotes the effect of cabbeling on the tendency equation of density and is generally positive [e.g., *Urakawa and Hasumi*, 2009]. Therefore, if the depth of water mass after sorting is deeper than the depth before sorting, cabbeling acts to produce APE. High latitudes are favorable for APE production by cabbeling because dense water masses exist near the surface.

4. Results

[12] Figure 1 shows meridional stream functions in the Atlantic and the Indo-Pacific. About 13.0 Sv of North Atlantic Deep Water is transported southward at the equator. The northward transport of AABW at 30°S is 6.3 Sv in the Atlantic. Estimates for these transports based on observations are 14 Sv and 4 Sv, respectively [*Schmitz*, 1995]. The northward cross-equatorial transport of Circumpolar Deep Water in the Indo-Pacific is 10.0 Sv. Overall, the fundamental structure of the MOC is well reproduced in this model, although the circulation associated with AABW formation is a little too strong

[13] The Antarctic Circumpolar Current is stronger in this model than in reality (205 Sv through the Drake Passage). This occurs because AABW is dominantly formed by parameterized open-ocean deep convection around Antarctica in this coarse resolution model, leading to uniform potential density profile from the top to bottom there and steeper density fronts than reality as discussed in *Urakawa and Hasumi*

Table 1. PE and BPE budgets in GW

PE Budget		Values (GW)	BPE Budget		Values (GW)
PE Tendency		+46	1st BPE tendency		+26
			2nd BPE tendency		−60
Surface buoyancy forcing (Φ_{b1})		+0	Surface buoyancy forcing (Φ_{b2})		−230
Energy conversion	TKE (Φ'_z)	+478	Irreversible mixing	Vertical (Φ_d^v)	+455
	MKE ($\overline{\Phi_z}$)	+229		Isopycnal (Φ_d^i)	+12
	EKE (Φ_z^{GM})	−380		Numerical (Φ_d^n)	+82
Nonlinearity of EoS	Vertical (Φ_c^v)	−10	Nonlinearity of EoS	Vertical ($\hat{\Phi}_c^v$)	+1
	Isopycnal (Φ_c^i)	−60		Isopycnal ($\hat{\Phi}_c^i$)	−169
	Numerical (Φ_c^n)	−39		Numerical ($\hat{\Phi}_c^n$)	−53
Vertical dependency of EoS (Φ_g)		−87	GM parameterization (Φ_{GM})		−69
Vertical isopycnal diffusion (Φ_{vi})		−72			
Convective adjustment (Φ_{ca})		−3	Convective adjustment ($\hat{\Phi}_{ca}$)		−0
Residual		+56	Residual		+29

[2010]. Such deficiencies are commonly found in coarse resolution models.

[14] Table 1 shows the global PE budget in this study. Three energy conversion terms are dominant: 478 GW of TKE (vertical diffusion) and 229 GW of MKE (mean flow) are converted to PE, and 380 GW of PE are converted to EKE (GM parameterization). *Munk and Wunsch* [1998] estimate the energy conversion from TKE to PE at 420 GW, which is smaller than our estimate. *Aiki and Richards* [2008] use an eddy-resolving model to estimate an energy conversion from PE to EKE. Their estimate is about 460 GW, which is larger than ours, while the estimate by *Urakawa and Hasumi* [2010] is 430 GW. Of the remaining PE, 109 GW is consumed by the nonlinear effects of the EoS, predominantly via isopycnal diffusion (60 GW). Cabbeling and thermobaricity are of similar magnitude in this latter term (30 GW by each; refer to the auxiliary material). The depth dependency of the EoS contributes significantly to consumption of PE (87 GW), as seen in *Urakawa and Hasumi* [2010]. The vertical component of isopycnal diffusion works to reduce PE by 72 GW owing to effective diapycnal flux in areas with steep isopycnal surfaces (isopycnal slopes for this diffusion are bounded by 0.01 in this study), which lowers the center of gravity and PE loss. The effect of convective adjustment is negligible at 3 GW. The residual of these terms is 56 GW, which is in good agreement with PE tendency term (46 GW).

[15] The BPE budget is shown on the right-hand side of Table 1. A major BPE source is irreversible mixing, with 549 GW converted from APE to BPE. A large fraction of that (455 GW) is accounted for by the effect of vertical diffusion. BPE of 230 GW is converted back to APE by surface buoyancy forcing, which explains less than half of the irreversible mixing effect. BPE of 221 GW is converted to APE by the nonlinear effects of the EoS, which is comparable to the effect of surface buoyancy forcing. The nonlinear effects due to isopycnal diffusion account for 169 GW of that, of which 89 GW results from cabbeling (refer to the auxiliary material). Similar to the result in *Hughes et al.* [2009], surface buoyancy forcing is balanced by irreversible mixing and the generation of APE by nonlinearities in the EoS. The GM parameterization, which is implemented in the model as layer thickness diffusion, combines with the vertical dependency of EoS leading to BPE loss of 69 GW. The residual of these fluxes in and out of BPE is +29 GW and is almost in balance with the "conventional" BPE tendency (first term in equation (3)). An additional BPE tendency term (second integral in equation (3)) amounts to −60 GW, which is relatively small compared to other terms in the BPE budget.

[16] The total energy fluxes caused by the nonlinear effects of the EoS result in a net sink from PE of 109 GW , but conversion from BPE to APE occurs at a rate of 221 GW. The PE sink is dominated by the effect of isopycnal diffusion, which is large in the Southern Ocean (Figure 1c; its effect on density tendency is shown in the auxiliary material), where intense thermal and haline fronts exist. Its effects extend to the deep ocean, and the contour line of $-2\,\mathrm{Wm}^{-2}$ almost reaches a depth of 3000 m at 45°S. Most of the BPE fluxes caused by the nonlinearities of the EoS occur at shallow depths at higher latitudes and are larger than those in the PE budget because the magnitude of z^* is large there. So, the net effect from isopycnal diffusion in the APE budget, which is calculated by taking the difference between those in the PE and BPE budgets, has a large value near the surface (Figure 1d). It locally exceeds $140\,\mathrm{Wm}^{-2}$ in the Southern Ocean. Because the difference between z and z^* becomes small in the deep ocean, the nonlinear effects of EoS on the APE budget decrease there. However, the contour line of $2\,\mathrm{Wm}^{-2}$ reaches over 2000 m depth, and this APE production is not restricted to the shallow ocean. The net APE production rate due to the nonlinear effects from isopycnal diffusion amounts to 109 GW.

5. Summary and Conclusions

[17] In this letter, it is shown that densification upon mixing, due to the effects of the nonlinear EoS, results in a source of APE. This is consistent with the notion that cabbeling, which is a major component of the nonlinearity,

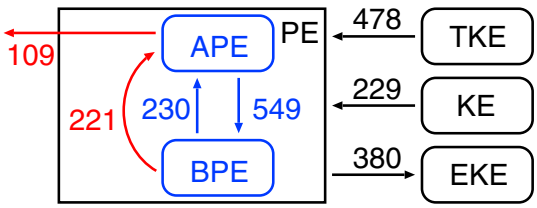

Figure 2. A schematic of major energy flows. Blue lines represent effects of surface buoyancy forcing (left) and irreversible mixing (right). Red lines denote the total (vertical, isopycnal, and numerical) nonlinear effects of the EoS. Power fluxes from Φ_g, Φ_{vi}, Φ_{ca}, and Φ_{GM} have been omitted.

is a source of density that can enhance the MOC. This resolves the apparent discrepancy that arises when considering the PE budget alone, where the nonlinear effects are a sink of energy (as shown in *Urakawa and Hasumi* [2010]). Figure 2 shows a schematic view of the energy budget of this model. The nonlinear effects lead to a sink of PE as already pointed out by earlier studies. PE of 109 GW is consumed in the model used in this study, which is significantly large compared to other terms in the PE budget. On the other hand, the nonlinear effects convert BPE to APE. BPE of 221 GW is converted to APE in this study. This energy conversion is almost equal to the energy conversion from BPE to APE by surface buoyancy forcing. The sum of these two terms is almost in balance with the conversion from APE to BPE due to irreversible mixing. The net nonlinear effects on the APE budget are a production of 112 GW, a substantial fraction of the total APE production. Although this study quantitatively shows the importance of the nonlinearity of the EoS in the APE budget, it is still an open question how much of this APE is converted to KE in the large scale and used for sustaining the MOC.

[18] **Acknowledgments.** This work was carried out during a visit by L.S.U. to ANU, supported by the Overseas Internship Program for Outstanding Young Earth and Planetary Researchers, Department of Earth and Planetary Science, the University of Tokyo. J.A.S. and A.M.H. were supported by Australian Research Council grant DPO986244, and A.M.H. was supported by the ARC Center of Excellence for Climate System Science (CE11E0098). Numerical computations were conducted using SR16000 at Information Technology Center, University of Tokyo. Our thanks go to Andreas Klocker, Fabien Roquet, Remi Tailleux, Trevor McDougall, and an anonymous reviewer, whose comments helped to improve the first draft of this paper.

[19] The Editor thanks Anand Gnanadesikan and Fabien Roguet for their assistance in evaluating this paper.

References

Aiki, H., and K. J. Richards (2008), Energetics of the global ocean: The role of layer-thickness form drag, *J. Phys. Oceanogr.*, *38*(9), 1845–1869.

Antonov, J. I., R. A. Locarnini, T. P. Boyer, A. V. Mishonov, and H. E. Garcia (2006), World Ocean Atlas 2005, Volume 2: Salinity, *NOAA Atlas NESDIS*, 62, 182pp.

Gnanadesikan, A., R. D. Slater, P. S. Swathi, and G. K. Vallis (2005), The energetics of ocean heat transport, *J. Climate*, *18*(14), 2604–2616.

Hasumi, H. (2006), CCSR Ocean Component Model (COCO) version 4.0, *CCSR report 25*, Center for Climate System Research, Univ. of Tokyo.

Hellmer, H. H., and A. Beckmann (2001), The Southern Ocean: A ventilation contributor with multiple sources, *Geophys. Res. Lett.*, *28*(15), 2927–2930.

Huang, R. X. (1998), Mixing and available potential energy in a Boussinesq ocean, *J. Phys. Oceanogr.*, *28*(4), 669–678.

Huang, R. X. (2005), Available potential energy in the world's ocean, *J. Mar. Res.*, *63*, 141–158.

Hughes, G. O., A. M. Hogg, and R. W. Griffiths (2009), Available potential energy and irreversible mixing in the meridional overturning circulation, *J. Phys. Oceanogr.*, *39*(12), 3130–3146.

Klocker, A., and T. J. McDougall (2010), Influence of the nonlinear equation of state on global estimates of dianeutral advection and diffusion, *J. Phys. Oceanogr.*, *40*(8), 1690–1709, doi:10.1175/2010JPO4303.1.

Kusahara, K., H. Hasumi, and T. Tamura (2010), Modeling sea ice production and dense shelf water formation in coastal polynyas around East Antarctica, *J. Geophys. Res.*, *115*, doi:10.1029/2010JC006133.

Locarnini, R. A., A. V. Mishonov, J. I. Antonov, T. P. Boyer, and H. E. Garcia (2006), World Ocean Atlas 2005, Volume 1: Temperature, *NOAA Atlas NESDIS*, *61*, 182pp.

Lorenz, E. N. (1955), Available potential energy and the maintenance of the general circulation, *Tellus*, *7*(2), 157–167.

McDougall, T. J. (1984), The relative roles of diapycnal and isopycnal mixing on subsurface water mass conversion, *J. Phys. Oceanogr.*, *14*(10), 1577–1589.

McDougall, T. J., D. R. Jackett, D. G. Wright, and R. Feistel (2003), Accurate and computationally efficient algorithms for potential temperature and density of seawater, *J. Atmos. Oceanic Technol.*, *20*(5), 730–741.

Munk, W., and C. Wunsch (1998), Abyssal recipes II: Energetics of tidal and wind mixing, *Deep-Sea Res. I*, *45*(12), 1977–2010.

Naveira Garabato, A. C., E. L. McDonagh, D. P. Stevens, K. J. Heywood, and R. J. Sanders (2002), On the export of Antarctic Bottom Water from the Weddell Sea, *Deep-Sea Res. II*, *49*, 4715–4742.

Orsi, A. H., G. C. Johnson, and J. L. Bullister (1999), Circulation, mixing and production of Antarctic Bottom Water, *Prog. Oceanogr.*, *43*, 55–109.

Röske, F. (2001), An atlas of surface fluxes based on the ECMWF re-analysis—a climatological dataset to force global ocean general circulation models, MPI-Rep. 323, Max-Planck-Institut für Meteorologie, Hamburg, Germany.

Saenz, J. A., A. M. Hogg, G. O. Hughes, and R. W. Griffiths (2012), Mechanical power input from buoyancy and wind to the circulation in an ocean model, *Geophys. Res. Lett.*, *39*, L13605, doi:10.1029/2012GL052035.

Schmitz, W. J. (1995), On the interbasin-scale thermohaline circulation, *Rev. Geophys.*, *33*(2), 151–173.

Tailleux, R. (2009), On the energetics of stratified turbulent mixing, irreversible thermodynamics, Boussinesq models and the ocean heat engine controversy, *J. Fluid Mech.*, *638*, 339–382, doi:10.1017/S002211200999111X.

Toggweiler, J. R., and B. Samuels (1998), On the ocean's large-scale circulation near the limit of no vertical mixing, *J. Phys. Oceanogr.*, *28*(9), 1832–1852.

Tsujino, H., H. Hasumi, and N. Suginohara (2000), Deep Pacific circulation controlled by vertical diffusivity at the lower thermocline depths, *J. Phys. Oceanogr.*, *30*, 2853–2865.

Urakawa, L. S., and H. Hasumi (2009), The energetics of global thermohaline circulation and its wind-enhancement, *J. Phys. Oceanogr.*, *39*(7), 1715–1728.

Urakawa, L. S., and H. Hasumi (2010), Role of parameterized eddies in the energy budget of the global thermohaline circulation: Cabbeling versus restratification, *J. Phys. Oceanogr.*, *40*(8), 1894–1901, doi:10.1175/2010JPO4361.1.

Urakawa, L. S., and H. Hasumi (2012), Eddy-resolving model estimate of the cabbeling effect on the water mass transformation in the Southern Ocean, *J. Phys. Oceanogr.*, *42*(8), 1288–1302.

Winters, K. B., P. N. Lombard, J. J. Riley, and E. A. D'Asaro (1995), Available potential energy and mixing in density-stratified fluids, *J. Fluid Mech.*, *289*, 115–128.